Effect of bed permeability and hyporheic flow on turbulent flow over bed forms

Blois, Gianluca; Best, James L.; Sambrook-Smith, Greg; Hardy, Richard J.

DOI:
10.1002/2014GL060906

Document Version
Publisher's PDF, also known as Version of record

Citation for published version (Harvard):
Blois, G, Best, JL, Sambrook-Smith, G & Hardy, RJ 2014, 'Effect of bed permeability and hyporheic flow on turbulent flow over bed forms', *Geophysical Research Letters*, vol. 41, no. 18, pp. 6435-6442. https://doi.org/10.1002/2014GL060906

AGU PUBLICATIONS

Geophysical Research Letters

RESEARCH LETTER
10.1002/2014GL060906

Key Points:
- Wall permeability allows mass and momentum exchanges at the interface
- Subsurface-surface flow exchange modifies flow structure in the bed form leeside
- Effects of permeability on morphology of coarse-grained bed forms

Supporting Information:
- Movie S1
- Movie S2

Correspondence to:
G. Blois,
blois@illinois.edu

Citation:
Blois, G., J. L. Best, G. H. Sambrook Smith, and R. J. Hardy (2014), Effect of bed permeability and hyporheic flow on turbulent flow over bed forms, *Geophys. Res. Lett.*, *41*, 6435–6442, doi:10.1002/2014GL060906.

Received 23 JUN 2014
Accepted 25 AUG 2014
Accepted article online 27 AUG 2014
Published online 26 SEP 2014

Effect of bed permeability and hyporheic flow on turbulent flow over bed forms

Gianluca Blois[1], James L. Best[1,2,3], Gregory H. Sambrook Smith[4], and Richard J. Hardy[5]

[1]Department of Geology and Department of Mechanical Science and Engineering, University of Illinois at Urbana-Champaign, Urbana, Illinois, USA, [2]Department of Geography and Department of Geographic Information Science, University of Illinois at Urbana-Champaign, Urbana, Illinois, USA, [3]Ven Te Chow Hydrosystems Laboratory, University of Illinois at Urbana-Champaign, Urbana, Illinois, USA, [4]School of Geography, Earth and Environmental Sciences, University of Birmingham, Birmingham, UK, [5]Department of Geography, Durham University, Durham, UK

Abstract This paper uses particle imaging velocimetry to provide the first measurements detailing the flow field over a porous bed in the presence of bed forms. The results demonstrate that flow downstream of coarse-grained bed forms on permeable beds is fundamentally different to that over impermeable beds. Most significantly, the leeside flow separation cell is greatly modified by jets of fluid emerging from the subsurface, such that reattachment of the separated flow does not occur and the Reynolds stresses bounding the separation zone are substantially lessened. These results shed new light on the underlying flow physics and advance our understanding of both ecological and geomorphological processes associated with permeable bed forms. Water fluxes at the bed interface are critically important for biogeochemical cycling in all rivers, yet mass and momentum exchanges across the bed interface are not routinely incorporated into flow models. Our observations suggest that ignoring such exchange processes in coarse-grained rivers may overlook important implications. These new results also provide insight to explain the distinctive morphology of coarse-grained bed forms, the production of openwork textures in gravels, and the absence of ripples in coarse sands, all of which have implications for modeling and prediction of sediment entrainment and flow resistance.

1. Introduction

Porous bed forms migrating over permeable beds (e.g., gravel/sand dunes) are ubiquitous in natural river environments and are of central importance in sediment transport and flow resistance [*García*, 2008], the generation of turbulence [*Best*, 2005], the formation of sedimentary structures [*Best*, 2005], solute transport, and hence the functioning of ecosystems [*Bardini et al.*, 2012; *Käser et al.*, 2013]. However, the study of flow-bed form interactions using either physical [*Best*, 2005] or numerical [*Grigoriadis et al.*, 2009; *Omidyeganeh and Piomelli*, 2013] models has typically assumed a simplified impermeable bed. It is clear, however, that this is a potentially flawed approach, as solute transport experiments indicate that up to one third of the total discharge can occur through bed sediments in coarse mountain streams [*Bencala and Walters*, 1983; *Böhlke et al.*, 2004]. Thus, significant exchanges of mass and momentum across permeable bed interfaces must occur and may have important ecological [*Bardini et al.*, 2012; *Hester et al.*, 2013] and morphodynamic implications [*Harrison and Clayton*, 1970]. Local pressure gradients are largely responsible for driving flow into and out of the bed. The steady component of such pressure gradients is induced by topography across scales (i.e., from grain-scale roughness to regional head differences). In some systems, bed forms are known to control a significant portion of such exchange [*Thibodeaux and Boyle*, 1987; *Lu and Chiew*, 2007]. Since the pioneering work of *Elliott and Brooks* [1997], who introduced the notion of advective pumping, the quantification of bed form-driven surface-subsurface exchange has relied on analytical models based upon time-averaged free-flow parameters. The nonhydrostatic pressure distribution induced by subaqueous bed forms at the water-bed interface has been traditionally used to develop analytical models linking mean free-flow velocity and seepage flow in two-dimensional bed form systems [*Packman and Brooks*, 2001; *Packman et al.*, 2000, 2004; *Marion et al.*, 2008]. However, while progress has been made into refining the original advective pumping model and extending it to more complex geometrical configurations [*Bardini et al.*, 2012; *Stonedahl et al.*, 2010], past research has largely neglected the nonlinearity of the turbulent flow *above* the bed. Recent numerical models typically treat the surface and subsurface flows as separate, assuming turbulent flows above the bed and Darcian flows beneath [*Cardenas and Wilson*, 2007a, 2007b; *Cardenas et al.*, 2008; *Jin et al.*, 2010; *Janssen*

et al., 2012]. The coupling is obtained through continuity on mean pressure terms, neglecting the existence of a transition region between the two regions, where unsteady and nonlinear interactions are reasonably expected. A detailed quantification of the flow field around bed forms resting on a permeable bed that would improve models of solute and particle transport [*Käser et al*., 2013; *Hester et al*., 2013; *Packman et al*., 2000], nutrient and carbon cycling [*Bardini et al*., 2012; *Jin et al*., 2010, 2011], and the spawning habitat of some fish [*Geist and Dauble*, 1998; *Baxter and Hauer*, 2000] in natural rivers is lacking. Additionally, the possible significance of hyporheic flow on the morphodynamics of the bed has been given little attention [*Harrison and Clayton*, 1970], yet may play a role in the entrainment and transport of sediment, and the subsequent production of bed relief. The present paper addresses the fundamental question of whether the flow field around a bed form in the presence of a permeable bed is significantly different to that of the commonly assumed impermeable bed. To answer this question, we report on a series of laboratory experiments using particle image velocimetry (PIV) to quantify the influence of subsurface flow on the flow field *above* a simplified, isolated, coarse-grained bed form fixed over a highly permeable bed. These experiments provide the first quantification of mass and momentum exchanges across the interface, highlighting the effects of permeability on turbulent stresses that have critical implications for solute fluxes and sediment stability at the interface, as well as the morphodynamics of bed forms.

2. Methods

Laboratory experiments were conducted in a specially constructed hyporheic flow flume that was 4.8 m long with a cross-sectional width, $W = 0.35$ m and height, $H = 0.60$ m. Additional details on the flume, including flow conditioning and instrumentation, can be found in *Blois et al*. [2012]. A permeable bed, which covered the entire length and width of the flume, was built using a simplified geometry comprising six layers of uniform spheres ($D = 0.038$ m diameter) that were rigidly fixed in a cubic arrangement. This bed was used to represent an idealized porous gravel bed. For the present study, both the thickness ($h_{bed} = 0.23$ m) of the permeable domain and water depths ($h_w = 0.19$ m) were kept constant, thus yielding a flow depth: bed thickness ratio, $h_w/h_{bed} \cong 0.8$.

The total flow discharge, Q_t, was measured using a magnetic flow meter in the return pipe to the pump. An ultrasonic Doppler velocimetry profiler was used to measure the mean velocity of the freestream flow, U_0. The mean flow discharge over the bed, Q_{stream}, was then estimated as $Q_{stream} = U_0 \cdot h_w \cdot W$. Due to constraints in the experimental setup, the measurement location was kept unchanged while the location of the bed form was varied to maximize the number of flow regions investigated. The bed form was placed in the flume at different distances from the inlet section where the flow was fully developed, in the range 2.2–3.6 m. The mean velocity U_0 was used to compute the freestream flow Reynolds number, $Re_s = U_0 \cdot h_w/\nu$ (where ν is the kinematic viscosity $= 1.004 \cdot 10^{-6}$ m$^2 \cdot$ s^{-1}) and the Froude number $Fr_s = U_0 \cdot (g \cdot h_w)^{-0.5}$ (where g is acceleration due to gravity $= 9.81$ m $\cdot$ s^{-1}). For the data reported herein, $Re_s = 2.5 \cdot 10^4$ and $Fr_s = 0.18$.

The flume was instrumented with two different particle imaging velocimetry (PIV) systems: (i) a standard PIV for above-bed measurements and (ii) an endoscopic PIV system (EPIV) for subsurface measurements. Above the bed, the flow was illuminated along the centerline of the test section by a 50 mJ Nd:YAG laser (Litron Lasers) and was imaged by a 4Mp camera (Redlake MotionPro Y5). Images were captured at both a low-frame rate (10 Hz), allowing sufficient images ($n = 2000$, time series was tested for stationarity) to be collected to obtain robust statistics, and at higher rates (80 Hz) to obtain time-resolved information. The laser light was introduced from the top of the flume as the water surface was relatively flat and no major refraction was present. In order to maximize the spatial resolution of the measurements, and at the same time cover a wide region (approximately 1.2 m) of flow including a region upstream (approximately 0.25 m) and downstream (approximately 0.6 m) of the dune, several ensemble-averaged flow fields were stitched together. For the subsurface flow, the EPIV system, based upon a two-borescope configuration [*Blois et al*., 2012], was employed with the seeding particles and image interrogation/validation schemes being the same as those used for the PIV.

Four experiments were conducted using three bed types: (i) an impermeable smooth bed, (ii) a porous bed, composed of cubically packed spheres, which was used to represent an idealized porous gravel bed, and (iii) an impermeable rough bed comprising hemispheres with diameter D. We examined flow over two idealized, asymmetric, triangular bed forms with the same cross section, 0.41 m in wavelength (λ), 0.056 m in amplitude (h), and with a leeside angle $\alpha_{lee} = 27°$, that represents a dune under the imposed flow depth [*Best*, 2005]

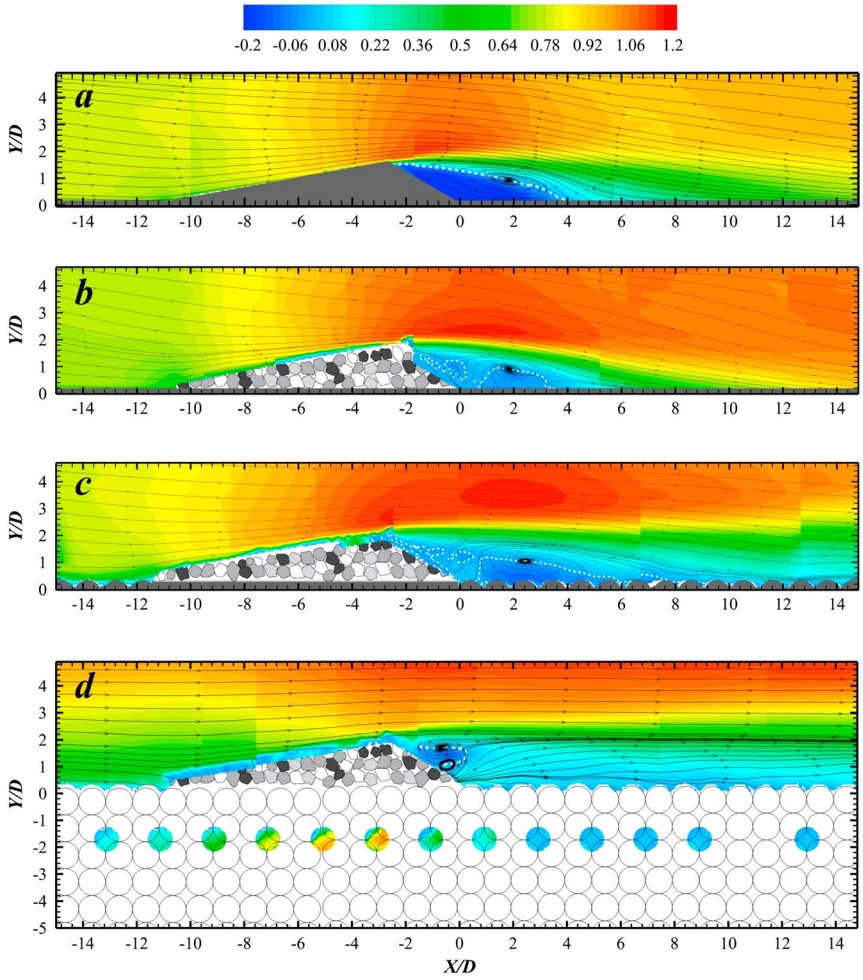

Figure 1. Distribution of normalized streamwise component of velocity (u/U_0) with superimposed streamlines for (a) impermeable dune over impermeable smooth bed (IDIB), (b) permeable dune over impermeable smooth bed (PDIB), (c) permeable dune over impermeable rough bed (PDIRB), and (d) permeable dune over permeable bed (PDPB). Bottom panel shows flow within the second pore space of the permeable bed. The white-dashed line represents location of zero streamwise velocity.

(flow depth at the bed form crest, $h_w = 0.19$ m; $h_w/h = 3.4$). The principal dune model comprised a mixture of 0.01 and 0.03 m diameter gravels, and flow over this bed form was examined for all three bed surfaces (rough and smooth impermeable, and rough permeable). Additionally, flow over an idealized, smooth, solid bed form was examined over a smooth impermeable bed to serve as a reference with past work on flow structure over asymmetrical impermeable bed forms [*Best*, 2005; *Bardini et al.*, 2012; *Cardenas and Wilson*, 2007a; *Janssen et al.*, 2012]. Flow above each bed form was quantified using PIV, while flow within 12 pore spaces within the bed was measured using EPIV [*Blois et al.*, 2012]. The present paper largely concentrates on flow *above* the bed.

3. Results

The flow field over both bed forms (permeable and solid) on both impermeable surfaces (smooth and rough; Figures 1a–1c, 2a–2c, and 3a–3c) shows characteristics similar to past work detailing flow structure over asymmetric bed forms [*Best*, 2005; *Cardenas and Wilson*, 2007a; *Omidyeganeh and Piomelli*, 2013]. Flow accelerates as it approaches the stoss side, separates at the crest, and eventually reattaches downstream. The mean streamwise velocity (Figures 1a–1c) reveals a zone of slower moving, recirculating flow in the dune leeside, which is characterized by one clockwise rotating vortex, with upward movement away from the bed near the dune leeface (Figures 2a–2c), and a clear nodal point in the streamline maps

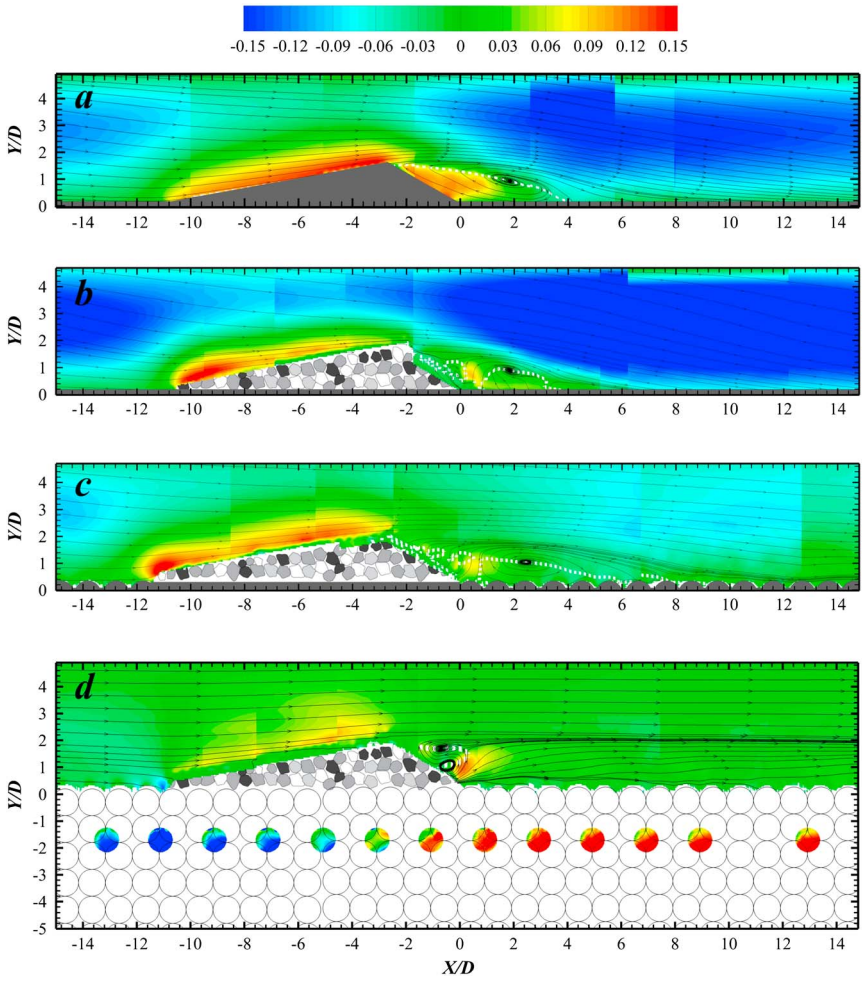

Figure 2. Distribution of normalized wall-normal component of velocity (v/U_0) with superimposed streamlines for (a) impermeable dune over impermeable smooth bed (IDIB), (b) permeable dune over impermeable smooth bed (PDIB), (c) permeable dune over impermeable rough bed (PDIRB), and (d) permeable dune over permeable bed (PDPB). Bottom panel shows flow within the second pore space of the permeable bed. The white-dashed line represents location of zero streamwise velocity.

(Figures 1a–1c and 2a–2c). The flow separation zone is bounded by a shear layer along which Kelvin-Helmholtz instabilities are generated [*Best*, 2005], with this layer being characterized by higher values of the wall-normal Reynolds stresses (Figures 3a–3c). This is confirmed by our time-resolved measurements (supporting information Movie S1) that show, in the case of the smooth solid bed form, that flow along the leeside shear layer is characterized solely by clockwise rotating vortices shedding from the bed form crest. The length of the separation zone is denoted by the mean location of the reattachment point, with this value being 4.2 *h*, 4.3 *h*, and 5.1 *h* for the dunes on an impermeable bed (Figures 1a–1c), showing similar values to past work [*Best*, 2005; *Omidyeganeh and Piomelli*, 2013] and demonstrating that the presence of roughness in either the bed (Figures 1c, 2c, and 3c) or bed form (Figures 1b, 2b, and 3b) has a limited influence on either the separation zone length or the principal characteristics of flow in the dune leeside. The introduction of permeability to the bed form (Figures 1b, 1c, 2b, 2c, 3b, and 3c) does produce some perturbation to the recirculating cell that loses some of its structural organization due to flow emerging from the bed form leeside. The addition of roughness to either the dune (Figures 1b and 2b) or underlying bed (Figures 1c and 2c) increases the Reynolds stresses slightly on the stoss side (Figures 3b and 3c) due to enhanced streamwise velocity fluctuations but decreases the Reynolds stresses in the leeside shear layer due to the damping of vertical velocities. Nevertheless, these phenomena have little influence on the overall structure of the leeside flow field.

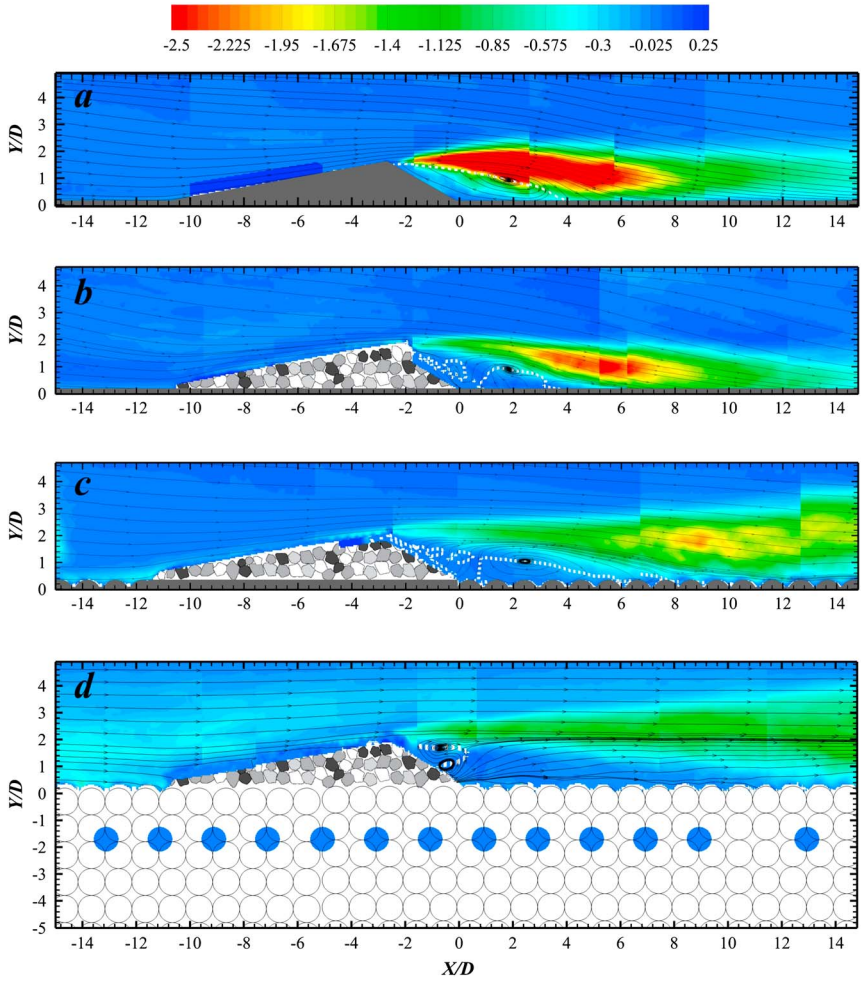

Figure 3. Distribution of normalized wall-normal Reynolds stresses ($u'v'/U_0^2$) with superimposed streamlines for (a) impermeable dune over impermeable smooth bed (IDIB), (b) permeable dune over impermeable smooth bed (PDIB), (c) permeable dune over impermeable rough bed (PDIRB), and (d) permeable dune over permeable bed (PDPB). Bottom panel shows flow within the second pore space of the permeable bed. The white-dashed line represents location of zero streamwise velocity.

However, the flow field associated with the dune on a permeable bed (Figures 1d and 2d) possesses radically different characteristics to those over the impermeable beds. Here, the low-momentum flow region in the leeside extends further downstream (Figure 1d), with strong jets of flow emerging from the subsurface, as shown by the positive vertical velocities in the pore space (Figure 2d (bottom) and supporting information Movie S2). Remarkably, the streamline map (Figure 1d) reveals that flow does not reattach in the dune leeside, at least within the region investigated, but rather is characterized by fluid moving away from the bed, which eventually moves parallel to the streamlines along the shear layer that originates at the dune crest and propagates downstream with a quasi-horizontal direction (Figures 1d and 2d). Flow within the leeside is replaced by two counter-rotating cells, with the jetting of flow from beneath the bed at the base of the dune lee slope generating a cell with an anticlockwise rotation (Figures 1d and 2d; supporting information Movie S2). The dynamics of the leeside flow are thus dramatically different from traditional models of leeside flow [*Best*, 2005; supporting information Movie S1]. Temporal changes in the size of the two counter-rotating flow cells (supporting information Movie S2) show an alternating pattern of growth of the basal cell, interaction with the cell nearest the bed form crest, and periodic shedding of these vortices from the leeside. Additionally, the wall-normal Reynolds stresses (Figure 3d) associated with the shear layer are lessened for the dune on a permeable bed (Figure 2d), and the zone of high Reynolds stress does not impinge on the bed as in the cases for the impermeable bed dunes. Upwelling flow in the leeside can be seen to be supplied by a positive vertical flow within the underlying pores in this region (Figures 1d, 2d, and 3d (bottom)), with

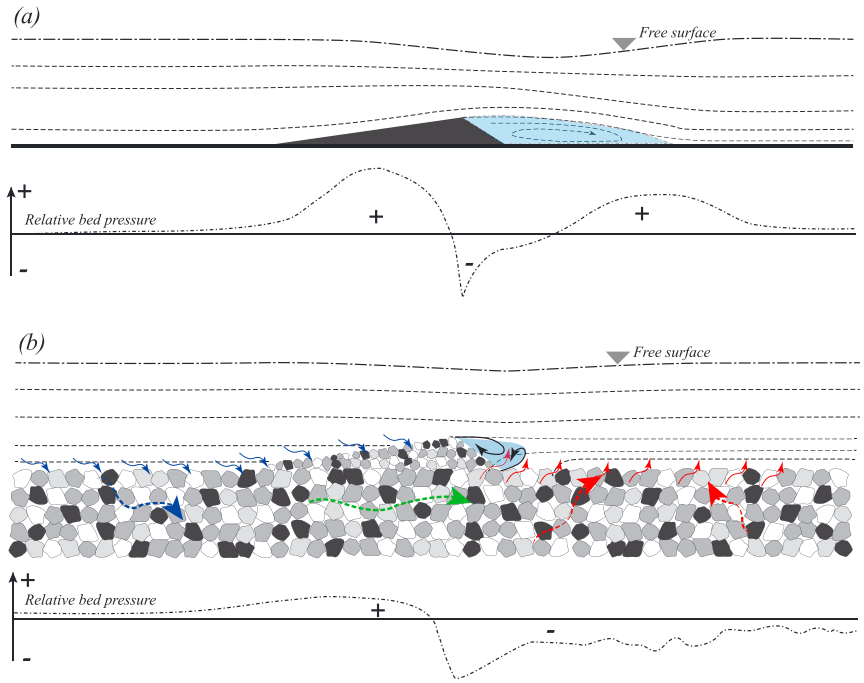

Figure 4. Schematic summary of flow around (a) reference case: impermeable bed form over impermeable smooth bed (IDIB), (b) natural bed form in coarse gravel bed: permeable bed form over permeable bed (PDPB). Streamlines over the bed form are shown, with the region in blue denoting the flow separation zone that is radically different in its shape and downstream extent over the PDPB. Note also the flow through the permeable bed form (dashed-large arrows) and upwelling hyporheic flow jets (small red arrowheads) in the leeside of the PDPB. The schematic bed pressure distribution associated with each bed configuration is shown to illustrate the potentially very different bed pressures associated with each bed.

subsurface flow downwelling on the stoss side and upwelling in the leeside (Figure 2d), as has been documented in previous studies of hyporheic flow and bed forms [*Cardenas and Wilson*, 2007a; *Janssen et al.*, 2012; *Hester et al.*, 2013; *Thibodeaux and Boyle*, 1987; *Jin et al.*, 2010; *Harrison and Clayton*, 1970].

4. Discussion

A number of important implications for natural aqueous geophysical flows arise from our results. Our observations suggest that modeling of hyporheic flow that is contingent upon a bed pressure distribution derived from the simulation of flow over an impermeable bed [*Cardenas and Wilson*, 2007a; *Janssen et al.*, 2012; *Hester et al.*, 2013; *Jin et al.*, 2010; *Cardenas et al.*, 2008] may be unrealistic in predicting the true nature of hyporheic flow beneath coarse-grained bed forms, whether these be pebble clusters, dunes, or larger bed forms [*Käser et al.*, 2013]. Recent work [*Janssen et al.*, 2012] has shown how parameterization of the eddy size associated with leeside flow separation is critical to correctly estimate the bed surface pressure distribution and nature of any subsurface pore water flow cells. Our results demonstrate that vertical fluid flow in the leeside of coarse-grained bed forms will be much different to that predicted in current models, and the absence of a reattachment region in the trough area, or on the stoss side of the downstream bed form, may generate lower positive pressures that will reduce downward hyporheic flow at this point. More realistic models should thus incorporate subsurface-surface flow feedbacks and their role in affecting the bed pressure distribution to simulate the movement of water, and particulates, into and out of the bed in the presence of bed form roughness.

The radically different flow field in the leeside of a bed form on a permeable bed outlined above, as compared to an impermeable bed, may also shed light on a number of unresolved sediment transport phenomenon that we briefly discuss here. As shown in Figure 3a, high Reynolds stresses are typically associated with the shear layer between the flow above the bed form and the leeside recirculation zone. Where this shear layer impinges on the bed at the point of reattachment, the high stresses exceed entrainment thresholds, generating

erosion and sediment transport over the stoss side of the next downstream bed form. However, for the permeable bed illustrated in Figure 3d, there is an overall reduction in the leeside stresses and critically no point of reattachment where the shear layer impacts the bed. Thus, the driving force for leeside scour is lessened or potentially removed by the influence of bed permeability. This may explain the observation of why the morphology of permeable coarse-grained bed forms, such as (i) "bars" in coarse sands that replace current ripples generated in finer sands [*Costello and Southard*, 1981] and (ii) gravel dunes [*Carling*, 1999] in their initial stages of formation, tend to be straight-crested, two-dimensional in planform, lack any distinct scour troughs, and may have an irregular wavelength [*Costello and Southard*, 1981].

The lack of flow reattachment may also provide an alternative explanation for the absence of current ripples in coarse sands at approximately $>$ 0.7 mm mean grain size [*Southard and Boguchwal*, 1973]. *Leeder* [1980] suggested that the grain roughness of coarse sands increased vertical mixing near the bed, thereby destroying the pressure gradients required to cause flow separation at the crest of grain defects on the bed, and thus preventing flow separation/reattachment forming regularly-spaced current ripples downstream. However, we speculate that if flow reattachment is prevented over initial grain defects on a plane bed due to the increasing influence of vertical jet flow as grain size and bed permeability increase, this provides a mechanism for generating bed forms that do not possess leeside scour at bed shear stresses just above the entrainment threshold. Thus, grain size and bed permeability may limit the formation of current ripples.

The vertical jet flow from the pore spaces of the bed up into the free flow may also play an important role in sediment suspension. For example, our results show vertical velocities within these jets of up to 0.4 ms^{-1}, sufficient to counteract the settling velocity of $\approx$ 3 mm diameter sediment and keep it in suspension. This mechanism could flush fines from the interstices of gravels into the free flow or prevent sediment from settling into these interstices during bed form migration. Such mechanisms may contribute to production of an openwork texture where gravels are depleted in fine-grained sediment [*Lunt and Bridge*, 2007]. The origin of such deposits is not fully understood, yet they play a major role in subsurface sediment heterogeneity and fluid flow in both the hyporheic zone [*Janssen et al*., 2012; *Hester et al*., 2013] and in water and hydrocarbon reservoirs [*Lunt and Bridge*, 2007].

In summary (Figure 4), our results demonstrate that flow in the leeside of coarse-grained bed forms on a permeable bed is fundamentally different to flow over an impermeable bed, the latter (Figure 4a) being the idealized case on which most models of bed form-generated hyporheic flow are currently based [*Cardenas and Wilson*, 2007a; *Cardenas et al*., 2008; *Jin et al*., 2010; *Janssen et al*., 2012; *Hester et al*., 2013]. Flow in the leeside of coarse-grained permeable bed forms (Figure 4b) may be expected to possess a greatly modified flow separation zone characterized by (i) a reattachment region that may either move further downstream or be absent, (ii) a substantial component of positive vertical velocity in the leeside near the bed interface, (iii) a shear layer that has lower Reynolds stresses than would be generated by a bed form overlying an impermeable bed, and consequently, (iv) an altered distribution of bed pressure over the bed form. These results have important implications for how we understand and model flows over and within coarse-grained sediment beds.

Acknowledgments

We acknowledge the Roscoe Jackson II Fellowship awarded to G.B. that allowed completion of this work, and the UK Natural Environmental Research Council for grant NE/E006884/1 awarded to GHSS and R.J.H. that allowed development of the EPIV system and HFF facility. We are also grateful to Marcelo García for provision of laboratory facilities that enabled this work. We thank the two anonymous reviewers for their helpful comments.

The Editor thanks two anonymous reviewers for their assistance in evaluating this paper.

References

Bardini, L., F. Boano, M. B. Cardenas, R. Revelli, and L. Ridolfi (2012), Nutrient cycling in bedform induced hyporheic zones, *Geochim. Cosmochim. Acta*, *84*, 47–61.

Baxter, C. V., and F. R. Hauer (2000), Geomorphology, hyporheic exchange, and selection of spawning habitat by bull trout (*Salvelinus confluentus*), *Can. J. Fish. Aquat. Sci.*, *57*, 1470–1481.

Bencala, K. E., and R. A. Walters (1983), Simulation of solute transport in a mountain pool-and-riffle stream: A transient storage model, *Water Resour. Res.*, *19*, 718–724.

Best, J. (2005), The fluid dynamics of river dunes: A review and some future research directions, *J. Geophys. Res.*, *110*, F04S02, doi:10.1029/2004JF000218.

Blois, G., G. H. Sambrook Smith, J. L. Best, R. J. Hardy, and J. R. Lead (2012), Quantifying the dynamics of flow within a permeable bed using time-resolved endoscopic particle imaging velocimetry (EPIV), *Exp. Fluids*, *53*, 51–76, doi:10.1007/s00348-011-1198-8.

Böhlke, J. K., J. W. Harvey, and M. A. Voytek (2004), Reach-scale isotope tracer experiment to quantify denitrification and related processes in a nitrate-rich stream, midcontinent United States, *Limnol. Oceanogr.*, *49*, 821–838.

Cardenas, M. B., and J. L. Wilson (2007a), Effects of current–bed form induced fluid flow on the thermal regime of sediments, *Water Resour. Res.*, *43*, W08431, doi:10.1029/2006WR005343.

Cardenas, M. B., and J. L. Wilson (2007b), Dunes, turbulent eddies, and interfacial exchange with permeable sediments, *Water Resour. Res.*, *43*, W08412, doi:10.1029/2006WR005787.

Cardenas, M. B., J. L. Wilson, and R. Haggerty (2008), Residence time of bedform-driven hyporheic exchange, *Adv. Water Resour.*, *31*, 1382–1386.

Carling, P. A. (1999), Subaqueous gravel dunes, *J. Sediment. Res.*, *69*, 534–545.

Costello, W. R., and J. B. Southard (1981), Flume experiments on lower-flow-regime bed forms in coarse sand, *J. Sediment. Petrol.*, *51*(3), 849–864.
Elliott, A. H., and N. H. Brooks (1997), Transfer of nonsorbing solutes to a streambed with bed forms: Laboratory experiments, *Water Resour. Res.*, *33*, 137–151, doi:10.1029/96WR02783.
García, M. H. (2008), Sediment transport and morphodynamics, in *Sedimentation Engineering: Processes, Measurements, Modeling, and Practice*, American Society of Civil Engineers Manuals and Reports on Engineering Practice No. 110, edited by M. H. García, chap. 2, pp. 21–163, American Society of Civil Engineers, Reston, Va.
Geist, D. R., and D. D. Dauble (1998), Redd site selection and spawning habitat use by fall chinook salmon: The importance of geomorphic features in large rivers, *Environ. Manage.*, *22*(5), 665–669.
Grigoriadis, D. G. E., E. Balaras, and A. A. Dimas (2009), Large-eddy simulations of unidirectional water flow over dunes, *J. Geophys. Res.*, *114*, F02022, doi:10.1029/2008JF001014.
Harrison, S. S., and L. Clayton (1970), Effects of ground-water seepage on fluvial processes, *Geol. Soc. Am. Bull.*, *81*, 1217–1226.
Hester, E. T., K. I. Young, and M. A. Widdowson (2013), Mixing of surface and groundwater induced by riverbed dunes: Implications for hyporheic flow definitions and pollutant reactions, *Water Resour. Res.*, *49*, 5221–5237, doi:10.1002/wrcr.20399.
Janssen, F., M. B. Cardenas, A. H. Sawyer, T. Dammrich, J. Krietsch, and D. A. de Beer (2012), A comparative experimental and multiphysics computational fluid dynamics study of coupled surface-subsurface flow in bedforms, *Water Resour. Res.*, *48*, W08514, doi:10.1029/2012WR011982.
Jin, G., H. Tang, B. Gibbes, L. Li, and D. A. Barry (2010), Transport of nonsorbing solutes in a streambed with periodic bedforms, *Adv. Water Resour.*, *33*(11), 1402–1416, doi:10.1016/j.advwatres.2010.09.003.
Jin, G., H. Tang, B. Gibbes, L. Li, and D. A. Barry (2011), Hyporheic flow under periodic bed forms influenced by low-density gradients, *Geophys. Res. Lett.*, *38*, L22401, doi:10.1029/2011GL049694.
Käser, D. H., A. Binley, and A. L. Heathwaite (2013), On the importance of considering channel microforms in groundwater models of hyporheic exchange, *River Res. Appl.*, *29*, 528–535, doi:10.1002/rra.1618.
Leeder, M. R. (1980), On the stability of lower stage plane beds and the absence of ripples in coarse sands, *J. Geol. Soc. London*, *137*, 423–430.
Lu, Y., and Y.-M. Chiew (2007), Suction effects on turbulence over a dune bed, *J. Hydraul. Res.*, *45*, 691–700.
Lunt, I. A., and J. S. Bridge (2007), Formation and preservation of open-framework gravel strata in unidirectional flows, *Sedimentology*, *54*, 71–87.
Marion, A., A. I. Packman, M. Zaramella, and A. Bottacin-Busolin (2008), Hyporheic flows in stratified beds, *Water Resour. Res.*, *44*, W09433, doi:10.1029/2007WR006079.
Omidyeganeh, M., and U. Piomelli (2013), Large-eddy simulation of three-dimensional dunes in a steady, unidirectional flow. Part 1: Turbulence statistics, *J. Fluid Mech.*, *721*, 454–483.
Packman, A. I., and N. H. Brooks (2001), Hyporheic exchange of solutes and colloids with moving bed forms, *Water Resour. Res.*, *37*, 2591–2605, doi:10.1029/2001WR000477.
Packman, A. I., N. H. Brooks, and J. J. Morgan (2000), Kaolinite exchange between a stream and streambed: Laboratory experiment and validation of a colloid transport model, *Water Resour. Res.*, *36*, 2363–2372, doi:10.1029/2000WR900058.
Packman, A. I., M. Salehin, and M. Zaramella (2004), Hyporheic exchange with gravel beds: Basic hydrodynamic interactions and bedform-induced advective flows, *J. Hydraul. Eng.*, *130*(7), 647–656.
Southard, J. B., and L. A. Boguchwal (1973), Flume experiments on the transition from ripples to lower flat bed with increasing sand size, *J. Sediment. Res.*, *43*, 1114–1121.
Stonedahl, S. H., J. W. Harvey, A. Wörman, M. Salehin, and A. I. Packman (2010), A multiscale model for integrating hyporheic exchange from ripples to meanders, *Water Resour. Res.*, *46*, W12539, doi:10.1029/2009WR008865.
Thibodeaux, L. J., and J. D. Boyle (1987), Bedform-induced convective transport in bottom sediment, *Nature*, *325*, 341–343.